Geophysical Research Letters

RESEARCH LETTER
10.1029/2021GL094599

The Impact of Sea-Ice Loss on Arctic Climate Feedbacks and Their Role for Arctic Amplification

Matthew Jenkins[1] and **Aiguo Dai**[1]

[1]Department of Atmospheric and Environmental Sciences, State University of New York, University at Albany, Albany, NY, USA

Key Points:

- Arctic lapse rate, Planck, and surface albedo feedbacks are greatly reduced without large sea-ice loss and surface warming
- Arctic positive lapse rate feedback likely results from enhanced surface warming caused by oceanic heating
- Winter oceanic heat release and summer albedo feedback are the main causes of Arctic amplification

Correspondence to:
A. Dai,
adai@albany.edu

Citation:
Jenkins, M., & Dai, A. (2021). The impact of sea-ice loss on Arctic climate feedbacks and their role for Arctic amplification. *Geophysical Research Letters*, *48*, e2021GL094599. https://doi.org/10.1029/2021GL094599

Received 29 MAY 2021
Accepted 17 JUL 2021

Abstract Sea-ice loss and radiative feedbacks have been proposed to explain Arctic amplification (AA)—the enhanced Arctic warming under increased greenhouse gases, but their relationship is unclear. By analyzing coupled CESM1 simulations with 1%/year CO_2 increases, we show that without large sea-ice loss and AA, the lapse rate, Planck, and surface albedo feedbacks are greatly reduced, while the positive water vapor feedback changes little. The positive Arctic lapse rate feedback, which results from enhanced surface warming rather than the high stability of Arctic air, and changes in atmospheric energy transport across the Arctic Circle are a result, not a cause, of AA; while the water vapor feedback also plays a minor role. Instead, AA results from enhanced winter oceanic heating associated with sea-ice loss that is aided by a positive surface albedo feedback in summer and positive cloud feedback in winter.

Plain Language Summary Increased atmospheric greenhouse gases cause large warming in the Arctic. The loss of sea-ice cover and positive climate feedbacks is proposed to explain the enhanced Arctic warming, but their relationship is unknown. We analyze two climate model simulations with 1%/year increases in atmospheric CO_2, one with dynamic sea ice and another with fixed sea ice, to quantify the impact of sea-ice loss on Arctic feedback processes. We find that without large sea-ice loss, Arctic lapse rate, Planck, and surface albedo feedbacks are reduced along with smaller Arctic warming. Melting sea ice minimally impacts the water vapor feedback but enhances the cooling effects of clouds in summer. Further, sea-ice loss increases surface absorption of solar energy in summer and the release of heat from the ocean to the atmosphere in winter, leading to enhanced Arctic warming in winter; while the contributions from the other feedbacks are likely small.

1. Introduction

Rapid warming in the Arctic region under increased greenhouse gases (GHG) is found in observations and model simulations (Barnes & Polvani, 2015; Screen & Simmonds, 2010a; Serreze & Barry, 2011; Serreze & Francis, 2006). The enhanced Arctic warming, termed Arctic amplification (AA), is largest from late autumn to early winter (A. Dai et al., 2019; Lu & Cai, 2009), and is strongest near the surface (especially over regions with sea-ice loss) and also in the lower-middle troposphere (Boeke & Taylor, 2018; A. Dai & Deng, 2021; A. Dai et al., 2019; Screen & Simmonds, 2010a). Proposed mechanisms of AA include heating from the Arctic Ocean during the cold season due to sea-ice loss (A. Dai et al., 2019; Screen & Simmonds, 2010a, 2010b), poleward energy transport (Cai, 2005), increased atmospheric water vapor and clouds that enhance downwelling longwave (LW) radiation to the surface (Burt et al., 2016), large surface absorption of shortwave (SW) radiation from the loss of sea ice (H. Dai, 2021; Graverson & Wang, 2009; Hall, 2004; Holland et al., 2006; Taylor et al., 2013; Zheng et al., 2019), and other processes.

Recent evidence shows that sea-ice loss is a key driver of AA (Boeke & Taylor, 2018; Chung et al., 2021; A. Dai et al., 2019; Screen & Simmonds, 2010b; Sejas et al., 2014; Taylor et al., 2018). During the summer, sea-ice melting exposes ocean waters, increasing ocean absorption of SW radiation and heat storage (Chung et al., 2021; H. Dai, 2021). As the atmosphere cools during the cold season, upward LW radiation, sensible (SH), and latent heat (LH) fluxes from unfrozen ocean surfaces warm the lower troposphere. As sea-ice melts under GHG-induced global warming, this seasonal process (i.e., warm-season absorption of SW radiation and cold-season heat release by the Arctic Ocean) is enhanced, leading to large AA during the cold season. When sea ice is fixed or completely melts away, changes in surface energy fluxes and AA are greatly reduced (A. Dai et al., 2019).

© 2021. American Geophysical Union. All Rights Reserved.

Previous studies suggest that climate feedback processes, particularly the lapse rate (LR) feedback, enhance Arctic surface warming (Goosse et al., 2018; Pithan & Mauritsen, 2014; Previdi et al., 2020; Stuecker et al., 2018). A positive LR feedback occurs when the surface and lower troposphere warm more than the middle-upper troposphere, thereby suppressing the top-of-the-atmosphere (TOA) LW cooling. It is suggested (Bintanja et al., 2011; Goosse et al., 2018; Pithan & Mauritsen, 2014) that the positive Arctic LR feedback stems from the high stability of Arctic air, which confines surface heating and warming locally; however, Boeke et al. (2020) found that the positive Arctic LR feedback depends more on surface warming patterns than atmospheric stability. This implies a greater influence by near-surface processes than stability on the Arctic LR feedback.

The importance of sea-ice loss and climate feedbacks as mechanisms of AA motivates the following questions: Does sea-ice loss amplify Arctic climate feedbacks and thus Arctic warming? And what climate feedbacks are a cause, not a result, of AA? We investigate the impact of sea-ice loss on Arctic surface albedo, water vapor, Planck, LR, and cloud feedbacks; and changes in atmospheric poleward heat (or energy) transport (APHT) and oceanic heat uptake (OHU) using two transient climate model simulations and radiative kernels.

2. Model Simulations and Analysis Methods

2.1. CESM1 Simulations

The simulations used here were taken from and described by A. Dai et al. (2019) and A. Dai and Song (2020). We used the Community Earth System Model version 1 (CESM1) (Hurrell et al., 2013) with the Community Atmosphere Model version 4 (CAM4) option. The atmospheric model was run with 2.5° lon × ~2.0° lat spacing with 26 vertical levels, and the sea-ice and ocean models were run with ~1.0° lon × 0.5° lat spacing. We compare two transient 235-years simulations to a 150-years preindustrial control run (CTL) with atmospheric CO_2 concentration fixed at 284.7 ppmv. Our first simulation involves 1%/year increases in atmospheric CO_2 with fully coupled, dynamic sea ice (referred to as 1%CO_2). The second simulation (referred to as FixedIce) is the same as the 1%CO_2 run, except that CTL-derived fixed sea-ice fraction (instead of internally calculated ice fraction) is used to compute ice and water fractions in calculations of the grid-box mean values for the ice-atmosphere, ocean-atmosphere, and ice-ocean energy, momentum, and mass fluxes poleward of 30°N. Sea ice evolves dynamically in the FixedIce simulation; however, due to the use of the fixed ice fraction in the flux calculations, Arctic sea ice decreases only slightly in FixedIce, mainly around current ice margins. However, the small internal sea-ice loss is not felt by the atmosphere and ocean in FixedIce, as fixed sea-ice cover was used in calculating all surface fluxes. We compare the CTL climatology (average of years 1–80) to the 20-years average around the second doubling (i.e., years 131–150) of atmospheric CO_2 from the 1%CO_2 and FixedIce simulations, but results around the first CO_2 doubling (i.e., years 61–80) are qualitatively similar. Given that the magnitude of AA varies seasonally, we calculate the feedbacks during boreal summer (June-July-August, JJA) and winter (December-January-February, DJF). In this study, the Arctic region is defined as 67°–90°N.

2.2. The Radiative Kernel Technique

We implemented the radiative kernel technique (Soden et al., 2008) to calculate the climate feedbacks from a TOA perspective. A radiative kernel is the TOA radiative flux change in response to a unit perturbation of a climate variable (e.g., temperature). We used the kernels developed by Pendergrass et al. (2018) with the CESM1 model. Radiative kernels mainly depend on the radiative transfer algorithm used to generate them and can be applied consistently across different simulations by models that use the same radiative transfer code (Soden et al., 2008), although the kernels from the same model are preferred due to differences in model climatology. Mathematically, a radiative kernel is the partial derivative of the TOA flux with respect to a perturbed climate variable. For example, the surface albedo kernel is $K_\alpha = \partial R / \partial \alpha$, where R is the net TOA radiative flux and α is the surface albedo. We interpolated the kernels from Pendergrass et al. (2018) onto our CESM1 grid. Radiative kernels have been implemented to assess the relationship between sea-ice loss and climate feedbacks in fully coupled model simulations (e.g., Boeke et al., 2020; Morrison et al., 2019); however, no one has used this technique for prescribed sea-ice simulations.

We used the kernels to calculate TOA radiative flux changes in response to perturbations in surface albedo (α), atmospheric specific humidity (q), surface temperature (T_s), and atmospheric temperature (T_a). The TOA flux change in response to changes in a given variable, such as surface albedo, is calculated as $\Delta R_\alpha = K_\alpha \times \Delta\alpha$, where ΔR_α is the TOA radiative flux perturbation due to changes in surface albedo, K_α is the surface albedo kernel, and $\Delta\alpha$ is the surface albedo change between the perturbed and control climatology. Feedbacks are typically normalized by the global or local surface temperature change (referred to as the feedback parameter) and are thus represented in units of W m^{-2} K^{-1} (Block et al., 2020; Crook et al., 2011). Here, we examine both the unnormalized and normalized TOA flux changes to quantify the feedbacks by dividing the TOA flux changes by the Arctic-mean surface air temperature (T_{as}) change, which is 4.94 K (1.45 K) for JJA and 14.5 K (4.94 K) for DJF in the 1%CO_2 (FixedIce) run.

To calculate the water vapor (Equation 1), Planck (Equation 2), and LR (Equation 3) feedbacks, the product of the kernel and change in the variable is integrated over the model pressure levels (Block & Mauritsen, 2013; Soden et al., 2008)

$$\Delta R_{WV} = \int_{p0}^{pTOA} K_w * \Delta \ln(q)\, dp, \tag{1}$$

$$\Delta R_{PL} = K_{Ts} * \Delta T_{as} + \int_{p0}^{pTOA} K_{Ta} * \Delta T_{as}\, dp, \tag{2}$$

and

$$\Delta R_{LR} = \int_{p0}^{pTOA} K_{Ta} * \left(\Delta T_a - \Delta T_{as}\right) dp, \tag{3}$$

where Δ represents the difference between the perturbed and control climatology. The emission of LW radiation by water vapor scales with the natural logarithm of q; therefore, we use $\ln(q)$ to calculate the water vapor feedback (Shell et al., 2008). The pressure level of the tropopause (p_{TOA}) is assumed to decrease linearly from 100 hPa at the Equator to 300 hPa at the poles to remove radiative effects from the stratosphere (Pendergrass et al., 2018; Pithan & Mauritsen, 2014).

We calculate the change in the cloud radiative effect (ΔCRE) to estimate the effect of clouds on the TOA energy budget. ΔCRE represents the change from the control to perturbed climatology in the difference between all-sky and clear-sky net TOA fluxes. Soden et al. (2008) showed that ΔCRE cannot represent the cloud feedback since surface albedo, water vapor, and temperature change together with cloud cover. Therefore, we compute the cloud feedback (Equation 4) as

$$\begin{aligned}\Delta R_c = \Delta CRE &- \left(K_\alpha - K_\alpha^c\right) * \Delta\alpha - \left(K_{Ts} - K_{Ts}^c\right) * \Delta T_{as} - \int_{p0}^{pTOA} \left(K_{Ta} - K_{Ta}^c\right) * \Delta T_a\, dp \\ &- \int_{p0}^{pTOA} \left(K_q - K_q^c\right) * \Delta \ln(q)\, dp - \left(G - G^c\right),\end{aligned} \tag{4}$$

where (K–K^c) or (G–G^c) is the all-sky minus clear-sky difference in the radiative kernels or GHG forcing using data from Pendergrass et al. (2018).

We also estimate changes in APHT across 67°N and Arctic OHU as they may also affect near-surface warming in the Arctic. The APHT change is computed as the change in the difference between Arctic-mean net surface (R_{SFC}) and net TOA fluxes (R_{TOA}), accounting for atmospheric energy storage change $\left(\partial E / \partial t\right)$: $\Delta APHT = \Delta(R_{SFC} - R_{TOA} + \partial E / \partial t)$, where $E = (1/g)\int_{p0}^{pTOA}(c_p T + Lq + gz)dp$ is the vertically integrated moist static energy from the surface to the tropopause, neglecting tiny kinetic energy (Trenberth & Solomon, 1994). The OHU is calculated as the change in the net surface energy flux ($R_{SFC} = netSW_{SFC} + netLW_{SFC} + SH + LH$) over ocean surfaces only. All the fluxes are positive downward (poleward for APHT). All the fluxes and feedbacks were calculated at each grid box, and then averaged over 67°–90°N using area as the weight.

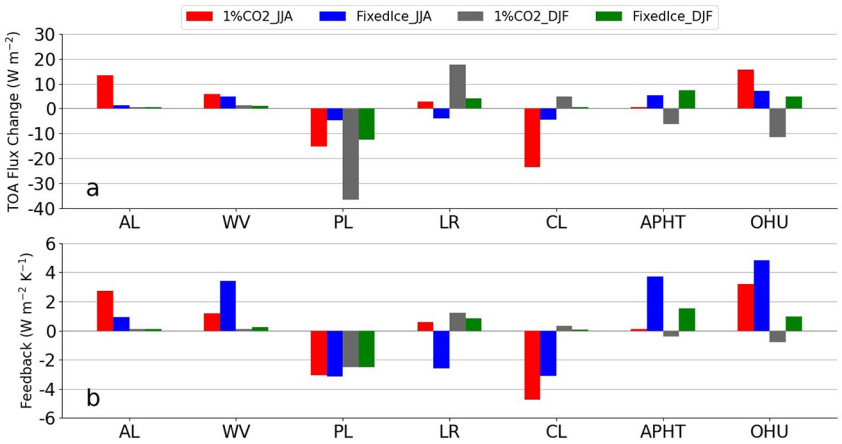

Figure 1. Changes (relative to the PI control climatology) in June-July-August (JJA) and December-January-February (DJF) mean top-of-the-atmosphere (TOA) radiative fluxes (a; in W m^{-2}) and feedback parameters (b; in W m^{-2} K^{-1}) in the CESM1 1%CO_2 and FixedIce simulations around the time of 4 × CO_2 (years 131–150) averaged over 67°–90°N due to the surface albedo (AL), water vapor (WV), Planck (PL), lapse rate (LR), and cloud (CL) feedbacks; and changes in atmospheric poleward heat transport (APHT, positive poleward) across 67°N, and Arctic ocean heat uptake (OHU). All fluxes are positive downward. "Heat" here includes all forms of energy.

3. Results

3.1. Impacts of Sea-Ice Loss on Radiative Feedbacks, APHT, and OHU

Figure 1a shows the unnormalized radiative flux changes averaged over the Arctic for JJA and DJF for the five feedbacks, APHT, and OHU from the 1%CO_2 and FixedIce experiments. Changes in the unnormalized surface albedo feedback and OHU are largest during JJA in the 1%CO_2 run, but are suppressed in FixedIce (Figure 1a), suggesting that large sea-ice loss enhances these processes. When sea ice melts, exposed ocean surfaces absorb more solar radiation than reflective ice surfaces, increasing summer OHU (Boeke & Taylor, 2018; H. Dai, 2021). Normalization by the Arctic-mean T_{as} change increases JJA values for FixedIce, but does not change the surface albedo feedback qualitatively (Figure 1b). The normalized OHU in JJA is slightly larger in FixedIce than in 1%CO_2.

Figure 2b shows the change in Arctic-mean temperature profiles in DJF and JJA for the two simulations. In FixedIce, the temperature change is approximately uniform from the near-surface to 400 hPa; while large sea-ice reductions (Figure 3) and increased ocean heat release (Figure 1) in the 1%CO_2 run greatly increase lower tropospheric (1,000–800 hPa) temperatures compared to the midupper troposphere (Figure 2b) in DJF. This bottom-heavy warming profile enhances the positive LR feedback in the Arctic. Further, the Arctic-mean temperature profile shows higher stability under FixedIce than in the 1%CO_2 run for both DJF and JJA (Figure 2a). Thus, atmospheric stability cannot explain the large seasonal differences in the LR feedback in the 1%CO_2 run or between the two simulations. Our FixedIce experiment shows that without large surface warming associated with sea-ice loss and ocean heat release, the tropospheric temperature warms fairly uniformly under a stable profile (Figure 2), leading to weak positive LR feedback in DJF (Figure 1a). Therefore, enhanced surface and lower tropospheric warming induced by sea-ice loss and associated ocean heat release is the primary cause of the positive winter Arctic LR feedback, consistent with Boeke et al. (2020) and Feldl et al. (2020). Our results also imply that a stable atmospheric temperature profile is not necessary for the existence of a positive LR feedback as thought previously (e.g., Pithan & Mauritsen, 2014), as long as there is strong surface heating (from the ocean) to cause elevated low-level warming.

The unnormalized Planck feedback is stronger in the 1%CO_2 run than in FixedIce for both DJF and JJA, especially for DJF (Figure 1a). In FixedIce, suppressed AA weakens the unnormalized Planck feedback for both seasons (Figure 1a), since a cool surface and lower troposphere reduce LW emissions. After the normalization, the Planck feedback is similar for both experiments and slightly stronger in JJA than DJF (Figure 1b). In other words, the changes in outgoing longwave radiation (OLR) per 1 K surface warming are similar among the two experiments for both seasons.

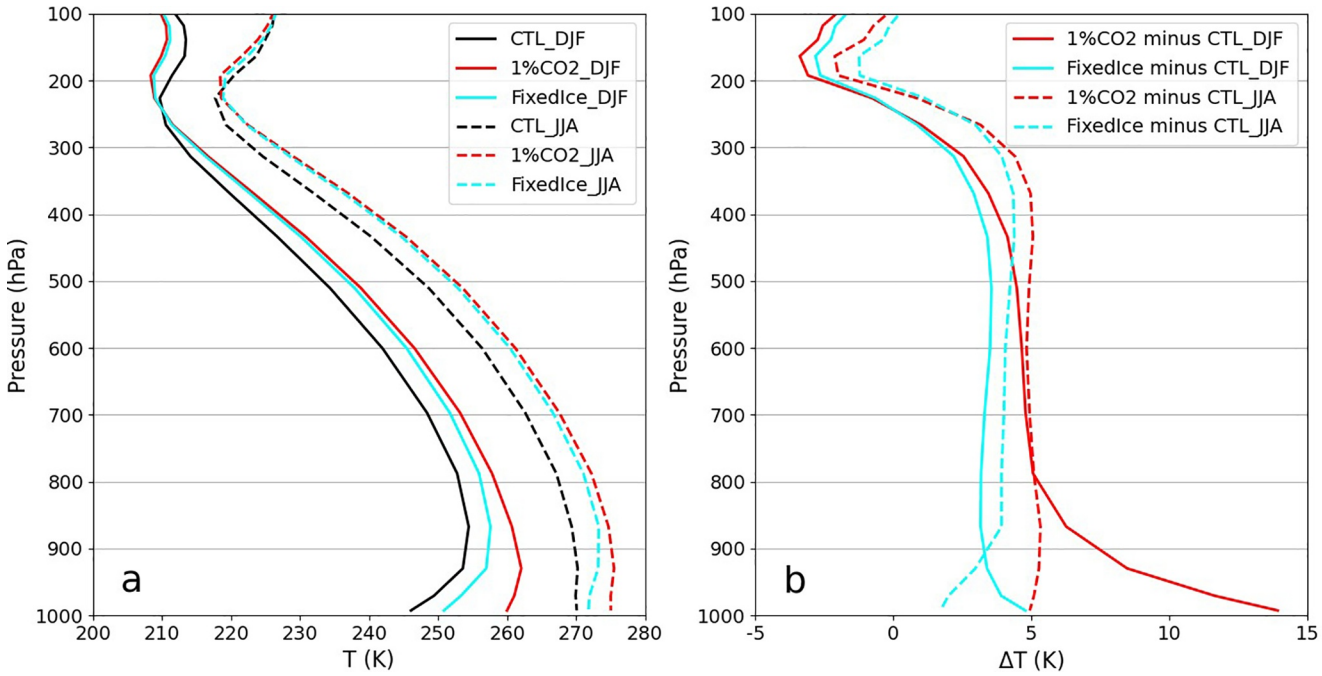

Figure 2. (a) December-January-February (DJF) (solid) and June-July-August (JJA) (dashed) Arctic (67°–90°N) mean temperature profiles (in K) for the CESM1 control run (CTL) climatology (black), and over years 131–150 of the 1%CO_2 (red) and FixedIce (blue) simulations. (b) Same as (a), but for the profile change relative the CTL climatology.

There is a strong negative cloud feedback in JJA in the 1%CO_2 run for normalized and unnormalized cases, and it is weaker under FixedIce (Figure 1). The cloud feedback becomes slightly positive in DJF in the 1%CO_2 run and closes to zero in FixedIce. Since SW radiation is low in DJF, cloud cover reduces OLR, resulting in a positive cloud feedback (Wetherald & Manabe, 1988). In JJA, clouds reflect SW radiation back to space, resulting in net cooling. For the 1%CO_2 run, the large albedo contrast between clouds and newly exposed ocean surfaces enhances the negative cloud feedback in JJA. In FixedIce, sea-ice changes little and the similar albedo between sea ice and clouds reduces the summer cooling effect of clouds. The stronger DJF positive cloud feedback in the 1%CO_2 run is due to its larger cloudiness increases (A. Dai et al., 2019).

Figure 1a shows that sea-ice loss has minimal impact on the unnormalized water vapor feedback consistent with Henry et al. (2021), with a slightly larger effect in JJA than DJF. Warmer temperatures during the summer allow the atmosphere to hold more water vapor, leading to a stronger warming effect by water vapor in JJA. Apparently, the logarithmic scaling of water vapor content in calculating its feedback (Equation 1) greatly reduces the difference in its impact on OLR between the two experiments. The normalized water vapor feedback is larger in FixedIce than the 1%CO_2 run for both JJA and DJF due to reduced surface warming in FixedIce (Figure 1b).

In the 1%CO_2 run, the APHT change in JJA is tiny, but becomes equatorward (i.e., negative) in DJF (Figure 1a). Given that sea-ice loss enhances Arctic-mean upward surface energy fluxes in DJF, the atmosphere displaces some of the excess energy to lower latitudes. In FixedIce, the atmosphere transports more energy poleward across the Arctic Circle than in CTL due to similar warming across northern latitudes in this experiment (A. Dai & Song, 2020). The direction of the APHT change at 67°N depends on the difference in Arctic surface and TOA energy flux changes, and it is equatorward when AA is large, consistent with Hwang et al. (2011).

3.2. Spatial Distributions of the LR, Planck, and Surface Albedo Feedbacks

Figure 3 shows the spatial distribution of the unnormalized LR feedback (i.e., TOA flux changes) for the 1%CO_2 and FixedIce experiments in DJF and JJA. For DJF, the largest TOA flux increase occurs over the

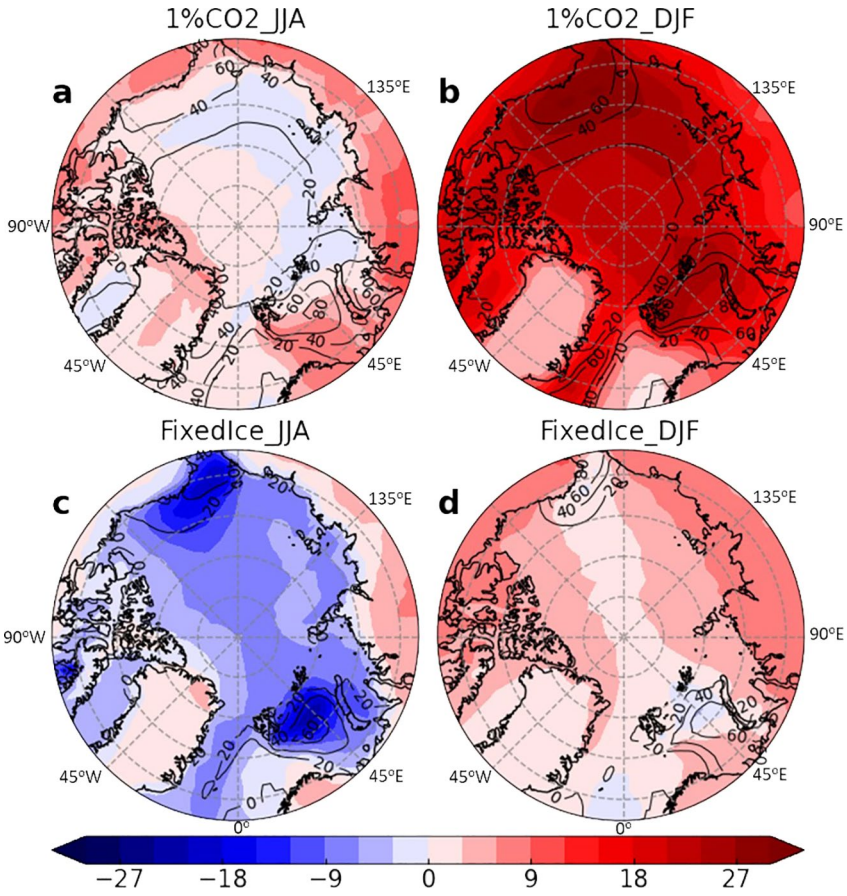

Figure 3. Changes (relative to the PI control climatology) over years 131–150 around 4 × CO_2 in the unnormalized lapse rate feedback (shading; in W m^{-2}, as reflected in the top-of-the-atmosphere (TOA) net energy flux) and sea-ice concentration (contours; in %; multiplied by −1) over 67°–90°N from the CESM1 (a and b) 1%CO_2 and (c and d) FixedIce simulations for (a and c) June-July-August (JJA), and (b and d) December-January-February (DJF) mean.

Chukchi and Barents-Kara Seas together with the largest sea-ice reductions in the 1%CO_2 run (Figure 3b), while the change is greatly reduced and slightly negative near the Barents Sea in FixedIce (Figure 3d). This suggests that the unnormalized LR feedback depends on the spatial patterns of sea-ice loss and the associated surface warming (Figures 3a and 3b), consistent with Boeke et al. (2020) and Feldl et al. (2020). In JJA, the LR feedback turns slightly negative over part of the Eastern Arctic Ocean for the 1%CO_2 run (Figure 3a) and substantially negative for the entire Arctic Ocean under FixedIce (Figure 3c). Note that sea ice also decreases along the ice margins in the Chukchi and Barents-Kara Seas by the time of quadrupling of atmospheric CO_2 in FixedIce (Figures 3c and 3d), but these ice losses are not felt by the atmosphere and ocean in this run.

The unnormalized negative Planck feedback is strongest in DJF and varies spatially in the 1%CO_2 run, with the largest flux changes over regions with large warming and sea-ice loss (i.e., the Chukchi and Barents-Kara Seas) (Figure 4a). The Planck feedback is weaker in JJA, especially over ocean surfaces due to small surface warming (not shown). Under FixedIce, the unnormalized Planck feedback is reduced substantially with little spatial variation for both DJF (Figure 4b) and JJA (not shown) compared to the 1%CO_2 run due to lack of large AA. The spatial distributions of the LR and Planck feedbacks highlight the importance of sea-ice loss and the resultant surface warming as a cause of these large climate feedbacks and AA.

The unnormalized surface albedo feedback is most active in JJA for the 1%CO_2 simulation and is suppressed under FixedIce (Figure 1a). In the 1%CO_2 run, large TOA flux changes due to decreased surface albedo occur

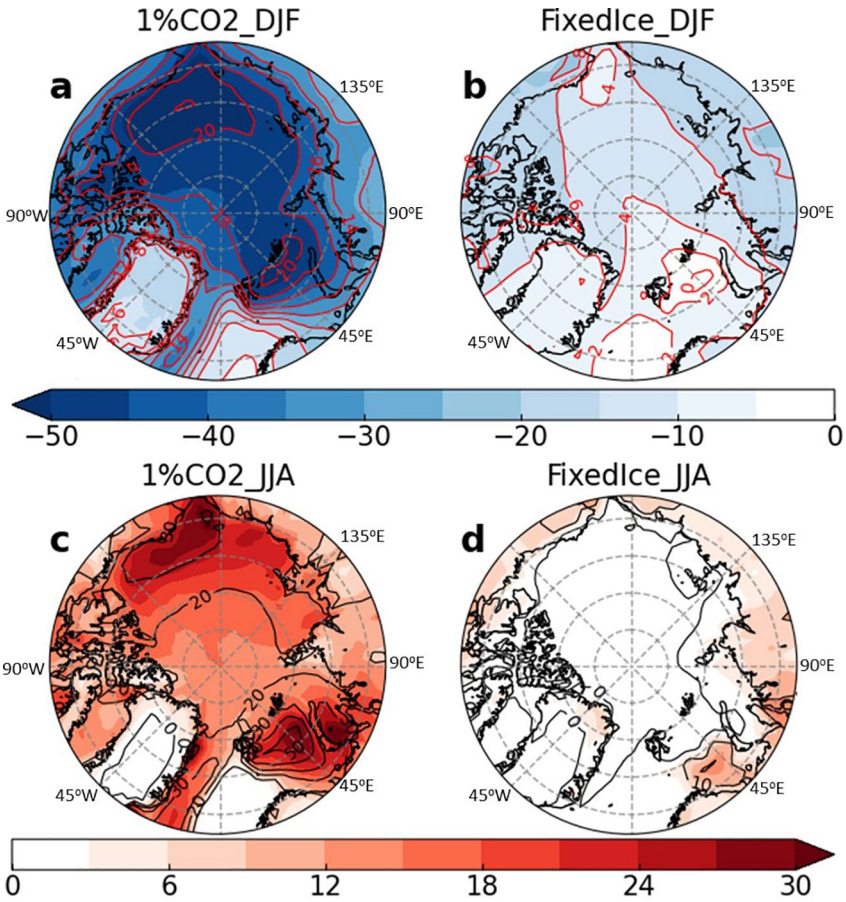

Figure 4. Top: Changes (relative to the PI control climatology) over years 131–150 around 4 × CO_2 in the December-January-February (DJF) unnormalized Planck feedback (shading; in W m^{-2}, as reflected in top-of-the-atmosphere (TOA) net energy flux) and surface air temperature (contours; in K) over 67°–90°N from the CESM1 (a) 1%CO_2 and (b) FixedIce runs. Bottom: Same as (a and b) but for changes in the JJA unnormalized surface albedo feedback (shading; in W m^{-2}) and surface albedo (contours; in %; multiplied by −1) from the CESM1 (c) 1%CO_2 and (d) FixedIce simulations.

over the Chukchi and Barents-Kara Seas (Figure 4c), while there are negligible reductions in surface albedo and little change in albedo feedback during JJA over much of the Arctic Ocean in FixedIce (Figure 4d).

4. Summary and Conclusions

We have examined the impact of sea-ice loss on Arctic climate feedbacks using two CESM1 simulations with 1%/year CO_2 increases with and without large sea-ice loss and AA. Our results suggest that the sign and magnitude of Arctic climate feedbacks depend on sea-ice loss and the resultant surface warming and albedo change. During DJF, enhanced upward LW, SH, and LH fluxes from the ocean in regions with reduced sea ice cause the surface and lower troposphere to warm faster than the upper troposphere in the Arctic, resulting in a large positive LR (lapse rate) feedback in the fully coupled simulation. In the FixedIce simulation with little sea-ice change, the enhanced fluxes and AA are reduced, leading to a weak LR feedback in DJF. Atmospheric stability differences between DJF and JJA or between the two simulations cannot explain the large differences in the LR feedback, suggesting that the high stability of Arctic air is not the main cause of the positive LR feedback in the cold season. This conclusion is consistent with Boeke et al. (2020) but contradicts the conventional notion (e.g., Bintanja et al., 2011; Pithan & Mauritsen, 2014). The unnormalized Planck feedback is strongly negative for the fully coupled simulation and is reduced under FixedIce for both DJF and JJA due to smaller surface warming, but it becomes similar after normalization by Arctic surface warming in the two simulations.

The surface albedo feedback is largest in JJA in the fully coupled simulation, especially in regions with large sea-ice loss. Low-albedo ocean surfaces absorb more SW radiation than reflective ice surfaces, increasing OHU in JJA. Under FixedIce, the surface albedo changes little, leading to small surface albedo feedback and small changes in summer OHU. In DJF, enhanced energy releases from the Arctic Ocean result in equatorward APHT across 67°N in the fully coupled simulation. The APHT becomes poleward under FixedIce due to suppressed surface energy fluxes. This suggests that Arctic OHU and APHT depend on sea-ice loss and the resultant Arctic surface energy fluxes (consistent with Hwang et al. [2011]), and cannot directly cause AA.

The cloud feedback is strongly negative during JJA and slightly positive in DJF in both experiments. In the fully coupled simulation, the negative cloud feedback in JJA results from the high albedo of clouds relative to ocean water surfaces, while in DJF the cloud's LW warming effect dominates. The DJF positive cloud feedback is larger in the fully coupled simulation than FixedIce, which is caused by increased cloudiness (A. Dai et al., 2019). Further, the unnormalized water vapor feedback does not show a strong dependence on sea-ice loss and is larger in JJA than DJF. The normalized water vapor feedback becomes larger under FixedIce than in the fully coupled due to reduced Arctic warming under FixedIce, implying that water vapor has a larger effect per unit warming when ocean-atmosphere energy fluxes are reduced. Therefore, the Arctic water vapor feedback is decoupled with sea-ice changes (consistent with Henry et al. [2021]) and cannot be a cause of AA.

Based on the above observations from our CESM1 simulations, we conclude that AA results from enhanced ocean heat release in the winter that is caused by sea-ice loss under GHG-induced warming, which leads to a positive surface albedo feedback in the summer and a moderate positive cloud feedback in the winter, both likely contributing to AA. All other feedbacks, including the water vapor and LR feedbacks, are not major causes of AA. In fact, the positive Arctic LR feedback is likely a result of AA. We realize that these are important statements about the mechanisms underlying AA that require validations using other model simulations.

Data Availability Statement

The model simulation data used in this study are available from https://doi.org/10.4121/14699514.

Acknowledgments
The authors thank Angeline Pendergrass and her coauthors for making the radiative kernels used in this study publicly available at https://doi.org/10.5065/D6F47MT6, and Dr. Tim Merlis and another anonymous reviewer for their constructive comments. This study was supported by the NSF (grants AGS-2015780 and OISE-1743738) and NOAA (grant NA18OAR4310425).

References

Barnes, E. A., & Polvani, L. M. (2015). CMIP5 projections of Arctic amplification, of the North American/North Atlantic circulation, and of their relationship. *Journal of Climate*, *28*, 5254–5271. https://doi.org/10.1175/JCLI-D-14-00589.1

Bintanja, R., Graversen, R. G., & Hazeleger, W. (2011). Arctic winter warming amplified by the thermal inversion and consequent low infrared cooling to space. *Nature Geoscience*, *4*, 758–761. https://doi.org/10.1038/ngeo1285

Block, K., & Mauritsen, T. (2013). Forcing and feedback in MPI-ESM-LR coupled model under abruptly quadrupled CO_2. *Journal of Advances in Modeling Earth Systems*, *5*, 676–691. https://doi.org/10.1002/jame.20041

Block, K., Schneider, F. A., Mülmenstädt, J., Salzmann, M., & Quaas, J. (2020). Climate models disagree on the sign of total radiative feedback in the Arctic. *Tellus A: Dynamic Meteorology and Oceanography*, *72*(1), 1–14. https://doi.org/10.1080/16000870.2019.1696139

Boeke, R. C., & Taylor, P. C. (2018). Seasonal energy exchange in sea ice retreat regions contributes to differences in projected Arctic warming. *Nature Communications*, *9*, 5017. https://doi.org/10.1038/s41467-018-07061-9

Boeke, R. C., Taylor, P. C., & Sejas, S. A. (2020). On the nature of the Arctic's positive lapse-rate feedback. *Geophysical Research Letters*, *48*, e2020GL091109. https://doi.org/10.1029/2020GL091109

Burt, M. A., Randall, D. A., & Branson, M. D. (2016). Dark warming. *Journal of Climate*, *29*, 705–719. https://doi.org/10.1175/JCLI-D-15-0147.1

Cai, M. (2005). Dynamical amplification of polar warming. *Geophysical Research Letters*, *32*, L22710. https://doi.org/10.1029/2005GL024481

Chung, E. S., Ha, K. J., Timmermann, A., Stuecker, M. F., Bodai, T., & Lee, S. K. (2021). Cold-season Arctic amplification driven by Arctic ocean-mediated seasonal energy transfer. *Earth's Future*, *9*, e2020EF001898. https://doi.org/10.1029/2020EF001898

Crook, J. A., Forster, P. M., & Stuber, N. (2011). Spatial patterns of modeled climate feedback and contributions to temperature response and polar amplification. *Journal of Climate*, *24*, 3575–3592. https://doi.org/10.1175/2011JCLI3863.1

Dai, A., & Deng, J. (2021). Arctic amplification weakens the variability of daily temperatures over northern middle-high latitudes. *Journal of Climate*, *34*, 2591–2609. https://doi.org/10.1175/JCLI-D-20-0514.1

Dai, A., Luo, D., Song, M., & Liu, J. (2019). Arctic amplification is caused by sea-ice loss under increasing CO_2. *Nature Communications*, *10*, 121. https://doi.org/10.1038/s41467-018-07954-9

Dai, A., & Song, M. (2020). Little influence of Arctic amplification on mid-latitude climate. *Nature Climate Change*, *10*, 231–237. https://doi.org/10.1038/s41558-020-0694-3

Dai, H. (2021). Roles of surface albedo, surface temperature and carbon dioxide in the seasonal variation of Arctic amplification. *Geophysical Research Letters*, *48*, e2020GL090301. https://doi.org/10.1029/2020GL090301

Feldl, N., Po-Chedley, S., Singh, H. K. A., Hay, S., & Kushner, P. J. (2020). Sea ice and atmospheric circulation shape the high-latitude lapse rate feedback. *npj Climate and Atmospheric Science*, *3*, 41. https://doi.org/10.1038/s41612-020-00146-7

Goosse, H., Kay, J. E., Armour, K. C., Bodas-Salcedo, A., Chepfer, H., Docquier, D., et al. (2018). Quantifying climate feedbacks in polar regions. *Nature Communications*, *9*, 1919. https://doi.org/10.1038/s41467-018-04173-0

Graverson, R. G., & Wang, M. (2009). Polar amplification in a coupled climate model with locked albedo. *Climate Dynamics*, *33*, 629–643. https://doi.org/10.1007/s00382-009-0535-6

Hall, A. (2004). The role of surface albedo feedback in climate. *Journal of Climate*, *17*, 1550–1568. https://doi.org/10.1175/1520-0442(2004)017<1550:TROSAF>2.0.CO;2

Henry, M., Merlis, T. M., Lutsko, N. J., & Rose, B. E. J. (2021). Decomposing the drivers of polar amplification with a single column model. *Journal of Climate*, *34*, 2355–2365. https://doi.org/10.1175/JCLI-D-20-0178.1

Holland, M. M., Bitz, C. M., & Tremblay, B. (2006). Future abrupt reductions in summer Arctic sea ice. *Geophysical Research Letters*, *33*, L23503. https://doi.org/10.1029/2006GL028024

Hurrell, J. W., Holland, M. M., Gent, P. R., Ghan, S., Kay, J. E., Kushner, P. J., et al. (2013). The community earth system model: A framework for collaborative research. *Bulletin of the American Meteorological Society*, *94*, 1339–1360. https://doi.org/10.1175/BAMS-D-12-00121.1

Hwang, Y., Frierson, D. M. W., & Kay, J. E. (2011). Coupling between Arctic feedbacks and changes in poleward energy transport. *Geophysical Research Letters*, *38*, L17704. https://doi.org/10.1029/2011GL048546

Lu, J., & Cai, M. (2009). Seasonality of polar surface warming amplification in climate simulations. *Geophysical Research Letters*, *36*, L16704. https://doi.org/10.1029/2009GL040133

Morrison, A. L., Kay, J. E., Frey, W. R., Chepfer, H., & Guzman, R. (2019). Cloud response to Arctic Sea ice loss and implications for future feedback in the CESM1 climate model. *Journal of Geophysical Research: Atmospheres*, *124*, 1003–1020. https://doi.org/10.1029/2018JD029142

Pendergrass, A. G., Conley, A., & Vitt, F. M. (2018). Surface and top-of-atmosphere radiative feedback kernels for CESM-CAM5. *Earth System Science Data*, *10*, 317–324. https://doi.org/10.5194/essd-10-317-2018

Pithan, F., & Mauritsen, T. (2014). Arctic amplification dominated by temperature feedbacks in contemporary climate models. *Nature Geoscience*, *7*, 181–184. https://doi.org/10.1038/NGEO2071

Previdi, M., Janoski, T. P., Chiodo, G., Smith, K. L., & Polvani, L. M. (2020). Arctic amplification: A rapid response to radiative forcing. *Geophysical Research Letters*, *47*, e2020GL089933. https://doi.org/10.1029/2020GL089933

Screen, J. A., & Simmonds, I. (2010a). Increasing fall-winter energy loss from the Arctic Ocean and its role in Arctic temperature amplification. *Geophysical Research Letters*, *37*, L16707. https://doi.org/10.1029/2010GL044136

Screen, J. A., & Simmonds, I. (2010b). The central role of diminishing sea ice in recent Arctic temperature amplification. *Nature*, *464*, 1334–1337. https://doi.org/10.1038/nature09051

Sejas, S. A., Cai, M., Hu, A., Meehl, G. A., Washington, W., & Taylor, P. C. (2014). Individual feedback contributions to the seasonality of surface warming. *Journal of Climate*, *27*, 5653–5669. https://doi.org/10.1175/JCLI-D-13-00658.1

Serreze, M. C., & Barry, R. G. (2011). Processes and impacts of arctic amplification: A research synthesis. *Global and Planetary Change*, *77*, 85–96. https://doi.org/10.1016/j.gloplacha.2011.03.004

Serreze, M. C., & Francis, J. A. (2006). The Arctic amplification debate. *Climatic Change*, *76*, 241–264. https://doi.org/10.1007/s10584-005-9017-y

Shell, K. M., Kiehl, J. T., & Shields, C. A. (2008). Using the radiative kernel technique to calculate climate feedbacks in NCAR's community atmospheric model. *Journal of Climate*, *21*, 2269–2282. https://doi.org/10.1175/2007JCLI2044.1

Soden, B. J., Held, I. M., Colman, R., Shell, K. M., Kiehl, J. T., & Shields, C. A. (2008). Quantifying climate feedbacks using radiative kernels. *Journal of Climate*, *21*, 3504–3520. https://doi.org/10.1175/2007JCLI2110.1

Stuecker, M. F., Bitz, C. M., Armour, K. C., Proistosescu, C., Kang, S. M., Xie, S. P., et al. (2018). Polar amplification dominated by local forcing and feedbacks. *Nature Climate Change*, *8*, 1076–1081. https://doi.org/10.1038/s41558-018-0339-y

Taylor, P. C., Cai, M., Hu, A., Meehl, J., Washington, W., & Zhang, G. J. (2013). A decomposition of feedback contributions to polar warming amplification. *Journal of Climate*, *26*, 7023–7043. https://doi.org/10.1175/JCLI-D-12-00696.1

Taylor, P. C., Hegyi, B. M., Boeke, R. C., & Boisvert, L. N. (2018). On the increasing importance of air-sea exchanges in a thawing Arctic: A review. *Atmosphere*, *9*, 41. https://doi.org/10.3390/atmos9020041

Trenberth, K. E., & Solomon, A. (1994). The global heat balance: Heat transports in the atmosphere and ocean. *Climate Dynamics*, *10*, 107–134. https://doi.org/10.1007/s003820050039

Wetherald, R. T., & Manabe, S. (1988). Cloud feedback processes in a general circulation model. *Journal of the Atmospheric Sciences*, *45*, 1397–1415. https://doi.org/10.1175/1520-0469(1988)045<1397:CFPIAG>2.0.CO;2

Zheng, J., Zhang, Q., Li, Q., Zhang, Q., & Cai, M. (2019). Contribution of sea ice albedo and insulation effects to Arctic amplification in the EC-Earth Pliocene simulation. *Climate of the Past*, *15*, 291–305. https://doi.org/10.5194/cp-15-291-2019